The Effect of Multiplanar Distal Radius Fractures on Forearm Rotation: *In Vitro* Biomechanical Study

Gillian S. Fraser, BSc, Louis M. Ferreira, BESc, James A. Johnson, PhD, Graham J.W. King, MD

Purpose Many patients develop distal radioulnar joint (DRUJ) pain and loss of forearm rotation after distal radial fractures. Residual distal radial deformity is one potential cause of DRUJ dysfunction; however, the parameters of distal radial fracture alignment that lead to an acceptable functional outcome are poorly defined in the literature.

Methods We used 8 fresh-frozen cadaveric specimens in this *in vitro* study to examine the effect of simulated distal radius fracture misalignment on forearm rotation. A distal radial osteotomy was performed just proximal to the DRUJ and a custom-made, 3-degrees-of-freedom modular implant designed to simulate distal radius fracture deformities was secured in place. This allowed for accurate simulation of dorsal angulation, dorsal translation, and radial shortening, both independently and in combination. We examined the effects of distal radius deformity in the setting of both an intact and sectioned triangular fibrocartilage complex.

Results Pronation was not significantly affected until dorsal angulation reached 30°. Dorsal translation of up to 10 mm or radial shortening up to 5 mm had no effect on forearm rotation. Combined deformities had a greater effect on forearm motion than isolated malpositions. Dorsal angulation of ≥20° combined with 10 mm of dorsal translation or 20° of angulation with 2.5 mm of radial shortening resulted in a significant decrease in forearm pronation. There was no effect of distal radial deformities, either isolated or combined, on the magnitude of forearm rotation after sectioning the triangular fibrocartilage complex.

Conclusions This study demonstrates that a broad range of distal radius fracture malpositions can be tolerated before a notable loss in forearm range of motion is evident. Combined deformities are more likely to result in a clinically important loss of forearm rotation, and this should be considered when choosing the optimal management of patients with displaced distal radial fractures. Disruption of the triangular fibrocartilage releases the tether on the DRUJ, allowing for preservation of forearm motion even in the setting of marked osseous deformities. *(J Hand Surg 2009;34A:838–848. Copyright © 2009 by the American Society for Surgery of the Hand. All rights reserved.)*

Key words DRUJ, wrist, Colles' fracture, fracture, kinematics.

FRACTURES OF THE distal radius are the most common fracture of both adults and children.[1–7] Malunions of the distal radius frequently occur[1,8] and often lead to residual pain, stiffness, and loss of function.[9] An increased incidence of arthritis at the distal radial ulnar joint (DRUJ) has been reported with healed angulated distal radial fractures.[10]

A number of clinical[11–15] and biomechanical[16–19] studies have examined various aspects of distal radial deformities and their influence on forearm motion; however, the parameters of an acceptable reduction remain poorly defined. Biomechanical studies have typically modeled isolated deformities of the distal radius; nevertheless, clinically it is combined deformities that

From the Bioengineering Research Laboratory, The Hand and Upper Limb Centre, St. Joseph's Health Care London; and the Departments of Biomedical Engineering, Surgery, and Medical Biophysics, The University of Western Ontario, London, Ontario, Canada.

Received for publication April 3, 2008; accepted in revised form February 10, 2009.

No benefits in any form have been received or will be received related directly or indirectly to the subject of this article.

Corresponding author: Graham J. W. King, MD, The Hand and Upper Limb Centre, St. Joseph's Health Care London, Room D0-202, 268 Grosvenor Street, London, Ontario N6A 4L6, Canada; e-mail: gking@uwo.ca.

0363-5023/09/34A05-0006$36.00/0
doi:10.1016/j.jhsa.2009.02.011

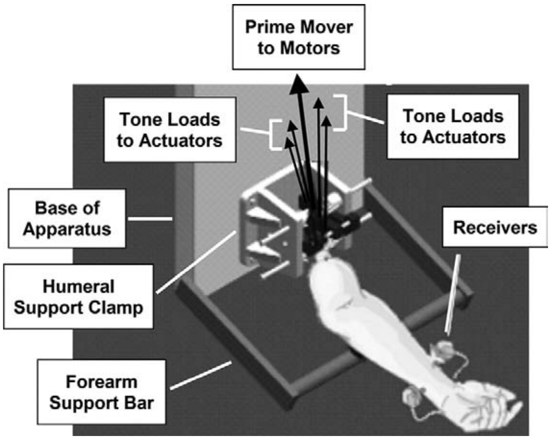

FIGURE 1: The upper extremity joint simulator. The distal humerus of the specimen is shown mounted to the upper extremity joint simulator by means of a clamp, attachment of cables from their respective muscles to dedicated pneumatic actuators, and the electromagnetic tracking system. Each actuator controls the load or displacement of its respective tendon. For clarity, not all cables are shown. An in-line load cell is connected to a servo motor and measures the forces in the prime mover for the motion of interest.

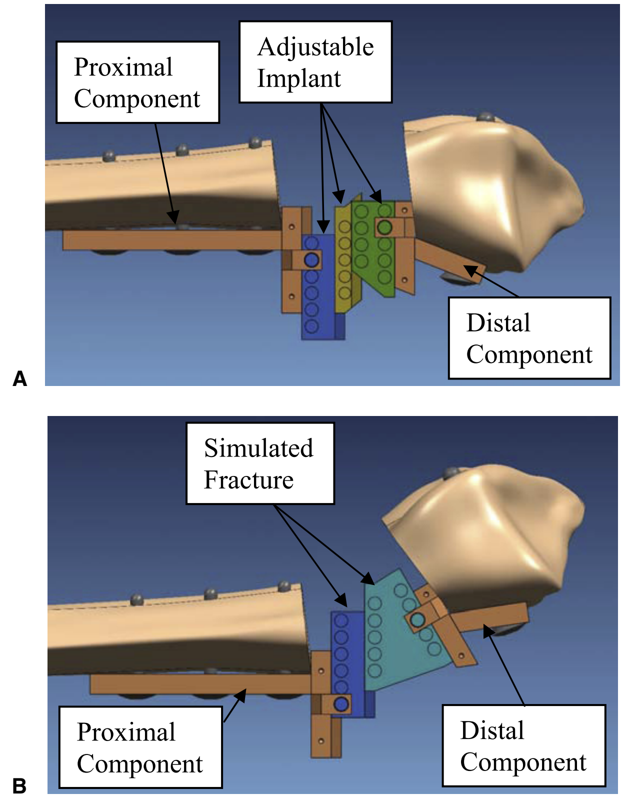

FIGURE 2: The 3-degrees-of-freedom adjustable implant employed to simulate distal radius fracture deformities *in vitro*. The implant consisted of distal and proximal components rigidly fixed to the underlying bone, and a removable appliance that generates the desired distal radius positioning **A**. By modifying the locking position and exchanging preformed angulation appliances, the fracture fixation device allowed for accurate adjustment of individual and combined deformities of dorsal angulation, dorsal translation, and radial shortening. **B** Thirty-degree dorsal angulation with 10-mm dorsal translation.

most commonly occur. There are no reported studies comprehensively evaluating the effect of both isolated and combined distal radial deformities on DRUJ function. Furthermore, the influence of triangular fibrocartilage complex (TFCC) rupture, which often occurs in association with distal radial fractures, has not been addressed in previous investigations.

The objective of this study was to develop an improved understanding of how varying degrees of isolated and combined distal radius deformities, with and without TFCC sectioning, affect forearm rotation using an *in vitro* cadaver-based model. Our hypotheses were that combined deformities of the distal radius would decrease forearm rotation more than isolated deformities, and that sectioning of the TFCC would allow for improved motion.

MATERIALS AND METHODS

Specimen preparation

Eight fresh-frozen upper extremities (77 ± 5 years, five female, two right) with a radial inclination of 23.3° (±2.8°), radial tilt of 11.5 (±1.1), and ulnar variance of 0.4 (±0.5) were thawed and studied in a previously described forearm testing apparatus.[20,21] Tendons of the biceps, supinator, pronator quadratus, pronator teres, triceps, flexor carpi ulnaris, flexor carpi radialis, extensor carpi ulnaris, and extensor carpi radialis longus were sutured to remotely located actuators via stainless-steel cables. To mimic the muscle lines of action, the sutures for the pronator teres and wrist flexors were routed through the humeral canal via Delrin sleeves (DuPont, Mississauga, ON) inserted into the medial supracondylar ridge. The sutures for the wrist extensors were routed through a sleeve in the lateral supracondylar ridge. Suture anchors were used at the radial origin of the pronator quadratus and supinator muscles, and their sutures were routed through Delrin sleeves at the ulnar insertion sites. Both sutures were directed through the medullary canal of the ulna exiting at the posterior olecranon.[12] The humerus was mounted in the motion simulator in a clamp with a freestanding bar to support the forearm in 90° of elbow flexion throughout testing (Fig. 1). Active pronation and supination were simulated by attaching the cables of the prime movers (pronator teres and biceps, respectively) to servo motors

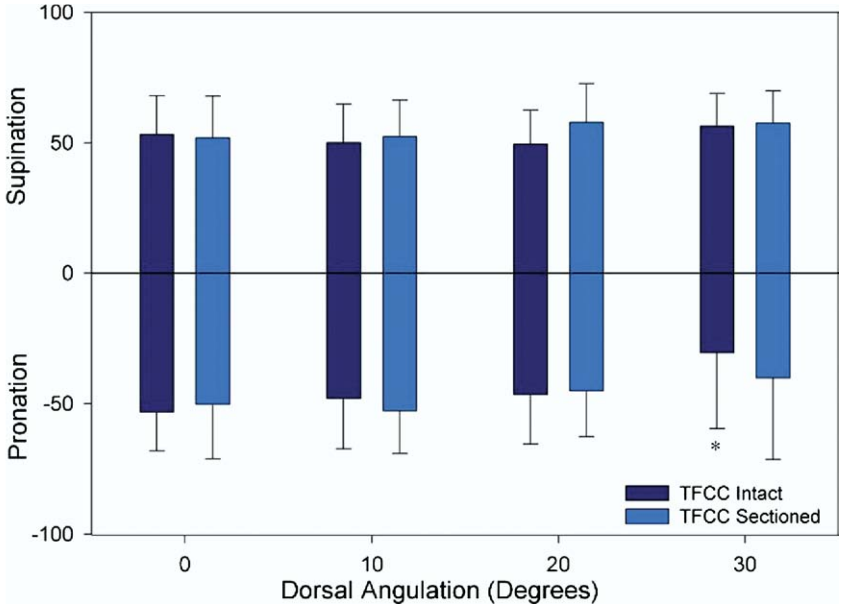

FIGURE 3: Effects of dorsal angulation of the distal radius on forearm pronation and supination motions for intact and sectioned TFCC. The mean +/− 1 SD of forearm rotation is shown. Increasing dorsal angulation resulted in a progressive loss of forearm pronation with the TFCC intact. This loss pronation was significant at 30° angulation ($p = .002$) for analysis of variance (*$p < .05$, compared with the native condition).

(SM2315D; Animatics, Santa Clara, CA) with 10:1 reduction gearboxes. The remaining cables were routed through an alignment system mounted to the testing apparatus and attached to dedicated pneumatic actuators as previously described.[20] Briefly, the load in each actuator was governed by a proportional pressure controller under computer control. Pronation was achieved by motor-based motion control of the pronator teres at a constant tendon velocity of 5 mm/s, while applying 44% of this load simultaneously to the pronator quadratus. Similarly, supination was accomplished by motion control of the biceps, while 33% of the load was apportioned to the supinator. This load distribution was based on published muscle activity as quantified by electromyography and the relative cross-sectional areas.[22–24] The triceps tendon was loaded with a constant force averaging 67.5 ± 4.6 N to prevent elbow flexion off the support bar during forearm rotation. Tone loads were applied to the wrist flexors (flexor carpi ulnaris = 9.1 ± 4.5 N, flexor carpi radialis = 13.5 ± 10.9 N) and extensors (extensor carpi ulnaris = 16.3 ± 9.2 N, extensor carpi radialis longus = 26.2 ± 7.9 N) to maintain neutral wrist flexion.[25] Receivers from the Flock of Birds (Ascension Technologies, Burlington, VT) electromagnetic tracking system were secured to the radius and ulna to quantify the 3-dimensional position and orientation of the radius relative to the ulna. The specimens were kept moist using 0.9% normal saline irrigation of the soft tissues, and by repeated closure of the skin during testing.

Testing procedure

A 3-degrees-of-freedom adjustable implant was employed to simulate distal radius fracture deformities *in vitro* (Fig. 2A). The implant consisted of distal and proximal components that are rigidly affixed to the proximal and distal bone segments and a removable central appliance that generates the desired distal radius positioning (Fig. 2B). The fracture fixation device allowed for accurate adjustment of individual and combined deformities of dorsal angulation, dorsal translation, and radial shortening. The native position of the distal radius was maintained during attachment of the adjustable implant. To ensure that the location of the osteotomy was consistent across specimens, a cutting guide contoured to the volar aspect of the distal radius was secured into position and the underlying bone was marked to indicate the location of the osteotomy. Using an oscillating saw, we removed a 20-mm segment of the volar radius 2 mm proximal to the DRUJ. The adjustable implant was positioned and secured to the proximal and distal radius using bone screws augmented with polymethylmethracrylate while leaving an intact dorsal bone bridge. Active and passive pronation and supination motions were simulated and kinematic data were recorded in

TABLE 1. Individual Effects of Dorsal Angulation on Degree of Forearm Rotation

	0°			10°			20°			30°		
	Pronation	Supination	n	Pronation	Supination	n	Pronation	Supination	n	Pronation	Supination	n
TFCC intact	53.3 ± 14.8	53.3 ± 14.8	8	48.0 ± 19.3	50.1 ± 14.8	8	46.5 ± 19.0	49.5 ± 13.1	8	30.5 ± 29.0*	56.4 ± 12.5*	7
TFCC cut	50.2 ± 20.9	51.9 ± 16.0	8	52.7 ± 16.3	52.4 ± 14.0	8	45.1 ± 17.6	57.8 ± 14.9	8	40.1 ± 31.2	57.5 ± 12.4	7

The mean ± 1 SD of the number of specimens (out of 8) able to achieve the deformity is represented as the number (n). Loss of pronation was noted with 30° of dorsal angulation or 10 mm of dorsal translation.
*p < .05.

this intact configuration. The dorsal bone bridge was then divided and the motion simulations were repeated to act as a control.

In the first phase of the study, the TFCC was left intact while we evaluated the effects of simulated distal radius deformities. We independently evaluated the conditions of 0°, 10°, 20°, and 30° of dorsal angulation from the original palmar tilt; 0.0, 2.5, 5.0, and 7.5 mm of radial shortening; and 0.0, 5.0, and 10.0 mm of dorsal translation, as well as in combinations of dorsal angulation with translation or shortening. Unlike radiographic parameters that are often employed clinically, in this study we defined radial shortening as a loss of length of the radius. Angulation was defined as per the orthopedic convention of determining where the apex of the deformity is, or from the position of normal volar tilt of the articular surface. Only dorsal translation deformities were evaluated in this study. Positive dorsal translation was defined as translating the distal radial fragment in a dorsal direction relative to its native alignment. Neutral forearm rotation was defined as halfway between maximum pronation and supination. This testing protocol was then repeated after we sectioned the TFCC, to examine the effect of a simulated ligament injury of the DRUJ in conjunction with distal radius deformities.

We determined repeatability of the measured kinematics from 10 successive trials and evaluated the standard deviation and mean at 5° increments across the trials, with the maximum coefficient of variation reported (a statistical representation of the dispersion of an experimental model expressed as a percentage of the ratio of the standard deviation to the mean). Reproducibility was quantified by performing 10 successive trials with the distal radius in neutral, then proceeding to a more aggressive 30° of dorsal angulation deformity, followed by repeating the neutral alignment. The coefficient of variation of the kinematics was calculated as an indication of the relative measure of the variation among trials.

Data analysis

We collected kinematic data and prime mover loads (via a cable in-line load cell) using custom-written software programmed in LabView 7.1 (National Instruments, Austin, TX). Upon completion of testing, the joints were dissected and digitization of anatomic landmarks was performed relative to the transmitter using a stylus with an attached tracking receiver.[20] To quantify the motion of the radius relative to the ulna, we established a clinically relevant joint coordinate system.[26] The ulnar coordinate system was determined by digi-

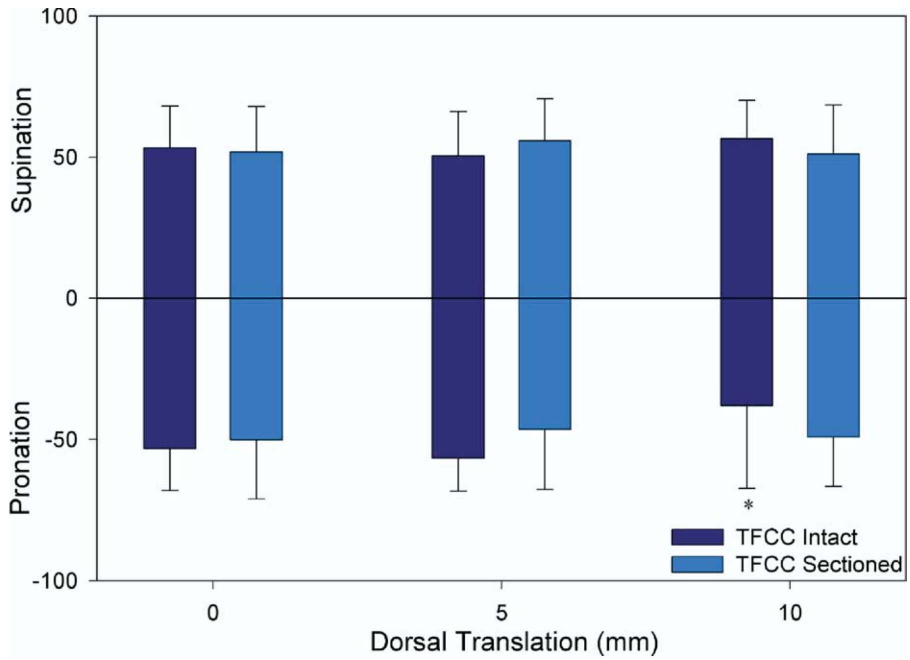

FIGURE 4: Effects of dorsal translation of the distal radius on forearm pronation and supination motions for intact and sectioned TFCC. The mean +/− 1 SD of forearm rotation is shown. Dorsal translation of 10 mm resulted in a significant (p = .03) loss of forearm pronation (p = .01).

TABLE 2. Individual Effects of Dorsal Translation on Degree of Forearm Rotation

	0 mm			5 mm			10 mm		
	Pronation	Supination	n	Pronation	Supination	n	Pronation	Supination	n
TFCC intact	53.3 ± 14.8	53.3 ± 14.8	8	56.7 ± 11.6	50.5 ± 15.7	8	38.1 ± 29.3*	56.6 ± 13.5	6
TFCC cut	50.2 ± 20.9	51.9 ± 16.0	8	46.5 ± 21.2	55.8 ± 14.8	8	49.1 ± 17.6	51.2 ± 17.2	8

The mean ± 1 standard deviation of the number of specimens (out of eight) able to achieve the deformity is represented as the number (n). Loss of pronation was noted with 30° of dorsal angulation or 10 mm of dorsal translation.
*p < .05.

tizing 2 bony landmarks, the ulnar styloid and the trochlear notch. A circle fit algorithm was applied to the trochlear notch and a vector between the ulnar styloid to the center of the circle, along the long axis of the ulna defined the pronation–supination axis with the ulnar styloid as the origin. A similar technique was conducted for the radial coordinate system by digitizing four points: the radial head, the dorsal and volar margins of the sigmoid notch, and the radial styloid. The origin of the radius was the average of the distal points. We determined the long axis of radius from the vector created from the origin at the distal end to the center of the sphere fit of the radial head. We developed software to analyze the motion of the radial coordinate system relative to the ulnar coordinate system.

All simulated fracture deformities were generated relative to the neutral intact state of each specimen. For example, a 10° increase in dorsal angulation referred to a 10° change from the original palmar tilt of the radius with the axis of the angulation at the volar cortex of the radius. The dependent (outcome variable) was the range of forearm rotation, determined from the maximum internal and external rotation of the radius about the long axis of the ulna. Neutral forearm rotation was defined for each specimen from the midpoint of maximum rotation at 90° of elbow flexion. Maximum forearm pronation and supination were quantified from the supinated and pronated starting positions, respectively, using a cutoff force of 60 N for the prime mover.

We compared the effect of radial deformity and TFCC state independently for pronation and supination by using a two-way repeated measures analysis of vari-

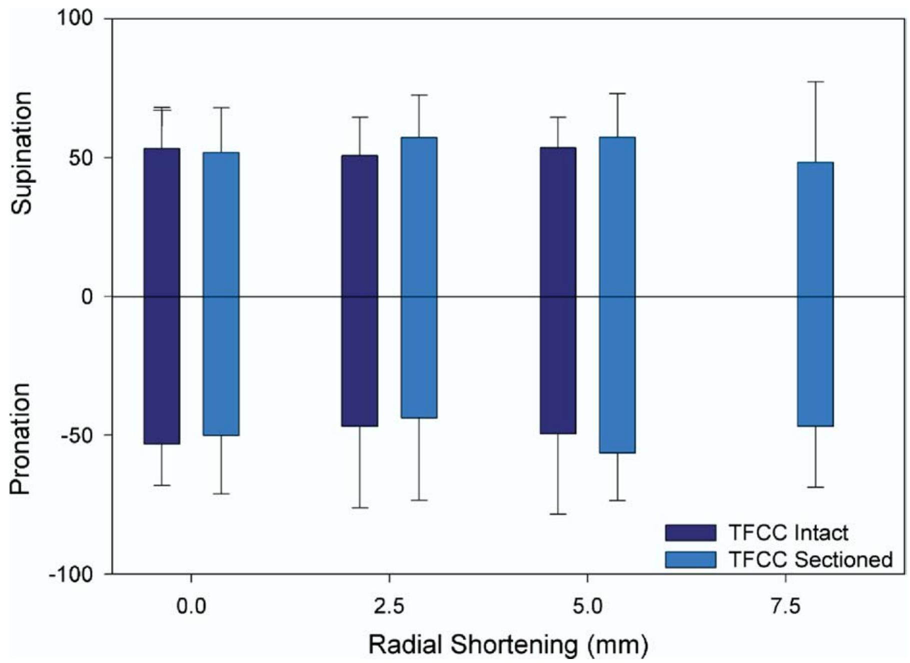

FIGURE 5: Effects of radial shortening of the distal radius on forearm pronation and supination motions for intact and sectioned TFCC. The mean +/− 1 SD of forearm rotation is shown. Radial shortening of 7.5 mm could not be achieved in any of the specimens until the TFCC was sectioned. There was no significant effect of radial shortening on forearm rotation ($p > .05$).

ance for the independent variables of alignment and TFCC status with post hoc Tukey tests ($\alpha = 0.05$). The influence of simulated distal radial deformity on the magnitude of forearm pronation and supination was examined separately.

Because all of the distal radial deformities could not be generated in all specimens due to tightness of the soft tissues, we conducted chi-squared analyses to determine whether there was a correlation between the magnitude of fracture deformity and ability to simulate the condition. The null hypothesis was accepted as true when the chi-squared values were >0.05.

RESULTS

The kinematics of the forearm were not significantly different before and after performing the osteotomy and securing the implant in neutral orientation ($p > .05$). The adjustable implant system was able to simulate the distal radial deformities of interest reliably in the specimens. The coefficients of variation were 0.34% and 0.41% for kinematics of pronation and supination, respectively, among the 10 repeatability runs. The reproducibility of active forearm kinematics in our testing simulator was also excellent, with 0.18% and 0.47% coefficients of variation for pronation and supination, respectively.

The average range of forearm rotation with the distal radius in the intact state was 106.5° ± 29.6° (range, 71° to 155°). Sectioning the TFCC increased the range of forearm rotation with the distal radius in the native position by 19.3° ± 21.9°.

Single deformities

We evaluated the effect of dorsal angulation, dorsal translation, and radial shortening on forearm motion as isolated deformities. Not all distal radial deformities could be simulated in all specimens because of the tightness of the soft tissues.

Dorsal angulation

Increasing dorsal angulation produced a significant reduction in forearm pronation when the TFCC was intact (Fig. 3, Table 1) ($p = .002$). Pronation was not statistically different from the native position until the magnitude of dorsal angulation reached 30°, which resulted in a mean 65% loss of pronation. Once the TFCC was sectioned, the range of motion was restored to the preinjured state. The magnitude of dorsal angulation had no significant effect on forearm supination ($p = .1$).

Dorsal translation

Increasing dorsal translation of the distal radial fragment decreased forearm pronation ($p = .03$) (Fig. 4).

Pronation was significantly different from the native position at 10 mm ($p = .04$), with the TFCC intact. Sectioning of the TFCC restored the range of motion to that of the native wrist ($p > .05$). In only 6 of 8 specimens were we able to simulate a 10-mm dorsal translation before TFCC sectioning because of soft tissue constraints (Table 2). There was no significant effect of dorsal translation on the range of forearm supination ($p = .2$).

Radial shortening

The radius could not be shortened more than 5 mm in any of the specimens until the TFCC was sectioned. This finding was significant using the chi-squared analysis ($p < .001$). Although we noted no statistically significant effect on forearm rotation ($p = .08$) with radial shortening of 5 mm, only half of the specimens could simulate 5 mm of radial shortening before the TFCC was sectioned (Fig. 5, Table 3). After this simulated ligament injury of the DRUJ, all but one specimen could achieve up to 7.5 mm shortening of the distal radius.

Combined deformities

Dorsal angulation and dorsal translation: We observed an increasing loss of forearm pronation as the magnitude of combined fracture malposition increased. Figure 6 demonstrates the effects of the combined variables for forearm pronation with the TFCC intact. Significant loss of rotation was not noted until 20° of dorsal angulation was combined with 10 mm of dorsal translation ($p = .03$), or 30° of dorsal translation was combined with 5 mm ($p = .04$) or 10 mm ($p = .001$) of dorsal translation. As the magnitude of fragment angulation and translation increased, fewer specimens were able to achieve these extreme positions, which decreased the available data (Table 4). Sectioning the TFCC led an increase in the amount of pronation achieved, also allowing more specimens to achieve more extreme malpositions.

Dorsal angulation and radial shortening: Isolated dorsal angulation of 30° caused a significant reduction in forearm pronation; yet, there was no effect on supination. When dorsal angulation was combined with radial shortening, significant loss in pronation occurred at angulations <30°. (Table 5, Fig. 7). Dorsal angulation of 20° combined with radial shortening of 2.5 mm resulted in a significant loss of pronation ($p = .04$).

DISCUSSION

Distal radial fracture displacement influenced forearm pronation greater than supination with intact soft tis-

TABLE 3. Individual Effects of Radial Shortening on Degree of Forearm Rotation

	0 mm			2.5 mm			5 mm			7.5 mm		
	Pronation	Supination	n	Pronation	Supination	n	Pronation	Supination	n	Pronation	Supination	n
TFCC intact	53.3 ± 14.8	53.3 ± 14.8	8	46.7 ± 29.4	50.7 ± 13.8	8	49.5 ± 28.9	53.5 ± 11.0	4	NA	NA	0
TFCC cut	50.2 ± 20.9	51.9 ± 16.0	8	43.7 ± 29.7	57.3 ± 15.2	8	56.4 ± 17.1	57.4 ± 15.6	7	46.8 ± 21.9	48.3 ± 29.0	7

The mean ± 1 SD of the number of specimens (out of 8) able to achieve the deformity is represented as the number (n). Loss of pronation was noted with 30° of dorsal angulation or 10 mm of dorsal translation.
NA, not achievable in any specimen.

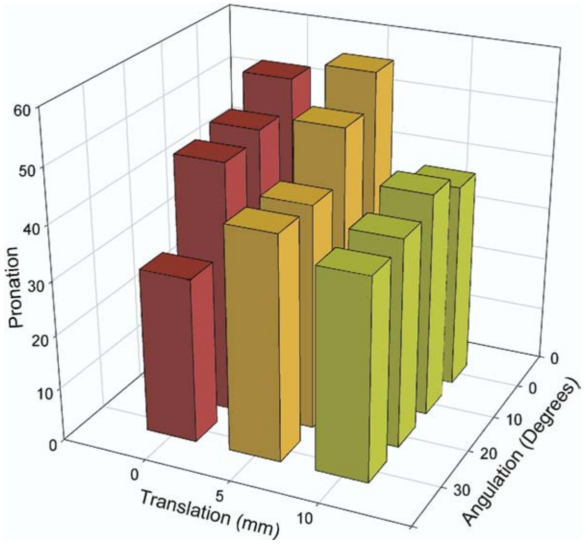

FIGURE 6: Mean pronation for dorsal angulation and dorsal translation of the distal radius with an intact TFCC. There was a progressive decrease in forearm pronation with increasing dorsal angulation and translation. This tended to be more pronounced with combined deformities; however, the least amount of forearm pronation was observed with 30° of dorsal angulation and 0 mm of translation.

sues. A significant loss of forearm rotation can be expected if distal radial fracture displacement reaches 30° of dorsal angulation or 10 mm of dorsal translation from the native position. Combined deformities had a greater effect on forearm rotation. Trends were noted with as little as 10° of dorsal angulation when combined with 10 mm of dorsal translation or 10° dorsal angulation when combined with 5 mm of radial shortening. In other words, these combined deformities resulted in a loss of 11.8° or 14.2° of pronation, respectively. This demonstrates the clinical importance of evaluating both distal fragment translation and angulation. The TFCC restrained the ability to simulate more severe fracture deformities, especially radial shortening. Because of soft tissue constraints about the wrist, radial shortening > 7.5 mm could only be achieved by sectioning the TFCC; therefore a major ligamentous injury of the DRUJ or fractures of the distal ulna or styloid should be suspected if such deformities are observed clinically. Schuind et al.[27] noted that there is some laxity in the TFCC; nevertheless, this study agrees with the findings of Adams [16] and af Ekenstam,[28] that malpositions of the distal radius alter the configuration of the TFCC and cause increased tissue tension, which likely limits forearm rotation. Sectioning the TFCC restored the kinematics to the preinjured state, eliminating any significant loss in rotation. This can likely be attributed to release of the tether on the DRUJ.

TABLE 4. Combined Effects of Radial Deformities (Dorsal Angulation and Dorsal Translation) on Degree of Forearm Rotation

	Intact		10° + 5 mm			20° + 5 mm			30° + 5 mm			10° + 10 mm			20° + 10 mm			30° + 10 mm		
	Pronation	Supination	Pronation	Supination	n	Pronation	Supination	n	Pronation	Supination	n	Pronation	Supination	n	Pronation	Supination	n	Pronation	Supination	n
TFCC intact	53.3 ± 14.8	53.3 ± 14.8	50.8 ± 16.0	48.4 ± 16.2	8	41.6 ± 20.4	53.7 ± 13.9	8	41.6 ± 19.3*	50.8 ± 13.0	7	41.5 ± 18.9	56.3 ± 10.2	6	38.6 ± 26.9*	53.9 ± 11.7	6	37.4 ± 15.0*	54.9 ± 12.6	5
TFCC cut	50.2 ± 20.9	51.9 ± 16.0	46.9 ± 20.8	55.7 ± 16.1	8	51.9 ± 15.5	53.5 ± 13.6	8	41.2 ± 23.0	60.3 ± 12.4	7	49.9 ± 14.7	47.3 ± 18.5	8	44.9 ± 17.3	53.4 ± 16.0	8	40.7 ± 27.3	52.1 ± 12.4	7

The number of specimens (out of 8) able to achieve the deformity is represented. Loss of pronation was noted when dorsal angulation was 20° combined with 10 mm of dorsal translation or 30° of angulation with any additional translation. Although not significant, this trend was noted with 10° angulation and 10 mm radial shortening or 20° angulation and 5 mm of radial shortening. With as little as 10° of dorsal angulation and 5 mm of radial shortening, a tendency to reduce pronation was observed. This observation was significant with 20° dorsal angulation and 2.5 mm of radial shortening.

*$p < .05$.

TABLE 5. Combined Effects of Radial Deformities (Dorsal Angulation and Radial Shortening) on Degree of Forearm Rotation

	Intact		10° + 2.5 mm			20° + 2.5 mm			30° + 2.5 mm			10° + 5 mm			20° + 5 mm			30° + 5 mm		
	Pronation	Supination	Pronation	Supination	n	Pronation	Supination	n	Pronation	Supination	n	Pronation	Supination	n	Pronation	Supination	n	Pronation	Supination	n
TFCC intact	53.3 ± 14.8	53.3 ± 14.8	51.9 ± 23.1	52.6 ± 13.0	7	35.3 ± 25.3	55.3 ± 11.3	7	37.4 ± 18.1	54.6 ± 11.3	6	39.1 ± 37.5	48.9 ± 28.2	6	35.2 ± 25.4	42.9 ± 22.6	5	15.4 ± 20.4*	33.8 ± 35.4*	4
TFCC cut	50.2 ± 20.9	51.9 ± 16.0	46.7 ± 17.7	57.5 ± 13.9	8	40.7 ± 32.8	58.4 ± 13.8	7	33.1 ± 35.2	60.4 ± 12.5	7	57.1 ± 16.5	58.3 ± 17.7	7	32.4 ± 38.8	61.7 ± 13.9	7	36.2 ± 38.2	56.6 ± 11.1	7

The number of specimens (out of 8) able to achieve the deformity is represented. Loss of pronation was noted when dorsal angulation was 20° combined with 10 mm of dorsal translation or 30° of angulation with any additional translation. Although not significant, this trend was noted with 10° angulation and 10 mm radial shortening or 20° angulation and 5 mm of radial shortening. With as little as 10° of dorsal angulation and 5 mm of radial shortening, a tendency to reduce pronation was observed. This observation was significant with 20° dorsal angulation and 2.5 mm of radial shortening.

*$p < .05$.

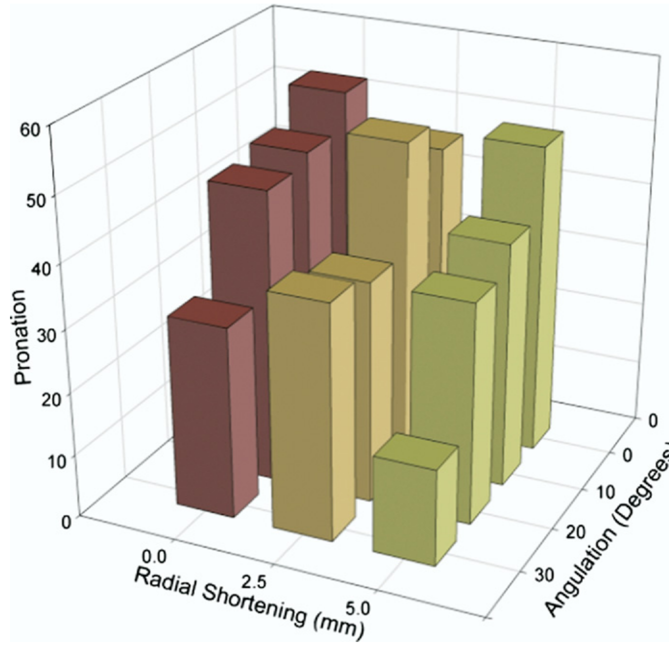

FIGURE 7: Mean pronation given the effects of dorsal angulation and radial shortening of the distal radius with an intact TFCC. There was a progressive decrease in forearm pronation with increasing dorsal angulation and radial shortening, which was more pronounced for combined deformities.

Bade et al.[29] noted similar findings in that dorsal angulation produced a considerable loss of pronation; however, supination losses were much less affected. Our *in vitro* results agree with this clinical experience, demonstrating a loss of pronation with preservation of supination in dorsally angulated, translated, and shortened distal radial fractures.

Although there are difficulties and inaccuracies in simulating joint motion and simulating relevant distal radial deformities *in vitro*, previous studies[16–19] have collectively demonstrated that increasing distal radial deformities decrease forearm rotation and lead to DRUJ incongruity. Each study used a unique methodology of motion simulation, data collection, and mechanism of osteotomy. The broad variation in conclusions of these studies demonstrates the difficulty in accurately simulating and evaluating the complex deformities of the distal radius. Furthermore, the lack of information regarding combined deformities, which commonly occur clinically, has not been reported to date.

Similar to the observations in the current study, Kihara et al.[17] reported that dorsal angulation of 30° significantly reduced the amount of forearm pronation; however, they also recorded a decrease in supination. The range of motion of the forearm was quantified using a tracking system with an external fixator to maintain the fragment deformity, and with forearm position created by deadweights applied to the biceps or pronator teres. That test method allowed for studying DRUJ stability only in static conditions. We speculate that differences noted resulted from the active forearm motion simulated in our study.

Bronstein et al.[19] concluded that radial shortening of 10 mm reduced the amount of forearm rotation; however, unlike the findings of the current study, dorsal tilt of 30° led to no significant forearm restriction in either pronation or supination. The testing apparatus applied a torque to the distal end of the fixator by a deadweight pulley, and measured rotation with a protractor. Each malaligned position of dorsal tilt, radial shift, or shortening was maintained in position by the external fixator pinned into the radial shaft and second metacarpal. The differences in the results of that study and the current investigation may be due to the rigidity of deformity simulation and the methodology of motion measurement.

Adams[16] found that radial shortening created the greatest disturbance in kinematics; dorsal angulation was intermediate and dorsal displacement showed the least change. Similar to our findings, they also experienced TFCC tightness occurring from the radial deformity, limiting the amount of radial malalignment that could be simulated. However, their biomechanical study used only one discrete position for each malunion (25° dorsal angulation, 5 mm radial shortening, or 50% dorsal displacement) and described the effect on the DRUJ in terms of TFCC strain and the instant center of rotation. Adams simulated forearm rotation from passively moving a pin inserted into the radius, whereas our forearm motion was a result of active motion created by forces applied to pronator teres, pronator quadratus, supinator, and/or biceps, as detailed previously. Their study involved disarticulating the wrist to allow for observation of DRUJ kinematics, which may have had a significant effect on DRUJ function given that some components of the TFCC were sectioned. Yet, even with these differences, similarities in findings were observed between the 2 studies.

Our study agrees with the finding of Hirahara et al.,[18] that the torque required to achieve full motion decreased after TFCC disruption, because we noted increased forearm rotation after sectioning these tissues. Similar to the current study showing that forearm supination was not affected by dorsal angulation up to 30°, they found that dorsal angulation had to exceed 30° before a significant increase in torque was required to achieve full supination. However, they did not measure a significant change in pronation until dorsal angulation reached 40°. Their study employed an external fixator and used identical force (3 kg to all dynamic muscles) to simulate active motion. Our study used load distribution based on muscle activity as quantified by electromyography and the relative cross-sectional areas. The alternative muscle loading ratios and the employment of an external fixator may have contributed to the differences noted. Use of external fixators to maintain stable fracture fixation was a limitation of these studies, because it was previously reported that considerable fragment motion can occur using external fixation to stabilize distal radial fractures.[25]

Few reports have detailed the load distributions on the wrist. Pogue et al.,[30] in a study of contact areas and pressures, found that dorsal angulation of 30° or 2 mm of radial shortening caused more concentrated loads in the scaphoid, lunate, or both. They also noted difficulty in obtaining displacements of the distal radius for shortening >4 mm or angulations exceeding 20° with the ulna styloid and the TFCC intact. We agree with those findings and suggest that in severely displaced fractures not associated with an ulna styloid fracture, a TFCC disruption should be suspected.

Weaknesses of this study are that that it was conducted on cadaveric specimens from elderly individuals. As such, there was a reduction in the available range of motion relative to younger specimens. Furthermore, the muscle loading that could be applied to create rotation was limited by the strength of the tendons, which further limited the range of motion. The anthropometric features of the specimens used within this study were within the normal population ranges. We could not study the influence of differences in the native anthropometric features of the distal radius on the response to distal radius deformities owing to the small sample size employed in this investigation.

Based on the results of the current investigation, surgeons evaluating distal radial deformities should carefully assess not only dorsal angulation, but also the concomitant presence of dorsal translation and radial shortening, which collectively can increase the dysfunction of the DRUJ manifested in this investigation as a loss of forearm pronation. The abnormal tension in the stabilizing soft tissues of the DRUJ likely would result in a loss of rotation as well as pain. Abnormal DRUJ joint kinematics and loading could also be expected to lead to the development of posttraumatic arthritis and early degenerative joint disease.

REFERENCES

1. Bacorn RW, Kurtzke JF. Colles' fracture; a study of two thousand cases from the New York State Workmen's Compensation Board. J Bone Joint Surg 1953;35A:643–658.

2. Court-Brown CM, Caesar B. Epidemiology of adult fractures: a review. Injury 2006;37:691–697.
3. Graff S, Jupiter J. Fracture of the distal radius: classification of treatment and indications for external fixation. Injury 1994;25(Suppl 4):SD14–SD25.
4. Levine AM. Fractures of the distal radius. In: Levine AM, ed. Orthopaedic knowledge update: trauma. Rosemont, IL: American Academy of Orthopaedic Surgeons, 1996:67–82.
5. Lindau T, Aspenberg P, Arner M, Redlundh-Johnell I, Hagberg L. Fractures of the distal forearm in young adults: an epidemiologic description of 341 patients. Acta Orthop Scand 1999;70:124–128.
6. Owen RA, Melton LJ III, Johnson KA, Ilstrup DM, Riggs BL. Incidence of Colles' fracture in a North American community. Am J Public Health 1982;72:605–607.
7. Mallmin H, Ljunghall S. Incidence of Colles' fracture in Uppsala: a prospective study of a quarter-million population. Acta Orthop Scand 1992;63:213–215.
8. Cooney WP III, Dobyns JH, Linscheid RL. Complications of Colles' fractures. J Bone Joint Surg 1980;62A:613–619.
9. Altissimi M, Antenucci R, Fiacca C, Mancini GB. Long-term results of conservative treatment of fractures of the distal radius. Clin Orthop Relat Res 1986;206:202–210.
10. Fernandez DL. Fractures of the distal radius: operative treatment. Instr Course Lect 1993;42:73–88.
11. Ishikawa J, Iwasaki N, Minami A. Influence of distal radioulnar joint subluxation on restricted forearm rotation after distal radius fracture. J Hand Surg 2005;30A:1178–1184.
12. Prommersberger KJ, Froehner SC, Schmitt RR, Lanz UB. Rotational deformity in malunited fractures of the distal radius. J Hand Surg 2004;29A:110–115.
13. McQueen M, Caspers J. Colles fracture: does the anatomical result affect the final function? J Bone Joint Surg 1988;70B:649–651.
14. Collins DC. Management and rehabilitation of distal radius fractures. Orthop Clin North Am 1993;24:365–378.
15. de Bruijn HP. Functional treatment of Colles fracture. Acta Orthop Scand Suppl 1987;223:1–95.
16. Adams BD. Effects of radial deformity on distal radioulnar joint mechanics. J Hand Surg 1993;18A:492–498.
17. Kihara H, Palmer AK, Werner FW, Short WH, Fortino MD. The effect of dorsally angulated distal radius fractures on distal radioulnar joint congruency and forearm rotation. J Hand Surg 1996;21A:40–47.
18. Hirahara H, Neale PG, Lin YT, Cooney WP, An KN. Kinematic and torque-related effects of dorsally angulated distal radius fractures and the distal radial ulnar joint. J Hand Surg 2003;28A: 614–621.
19. Bronstein AJ, Trumble TE, Tencer AF. The effects of distal radius fracture malalignment on forearm rotation: a cadaveric study. J Hand Surg 1997;22A:258–262.
20. Johnson JA, Rath DA, Dunning CE, Roth SE, King GJ. Simulation of elbow and forearm motion in vitro using a load controlled testing apparatus. J Biomech 2000;33:635–639.
21. Dunning CE, Gordon KD, King GJ, Johnson JA. Development of a motion-controlled in vitro elbow testing system. J Orthop Res 2003; 21:405–411.
22. Funk DA, An KN, Morrey BF, Daube JR. Electromyographic analysis of muscles across the elbow joint. J Orthop Res 1987;5:529–538.
23. Gordon KD, Dunning CE, Johnson JA, King GJ. Influence of the pronator quadratus and supinator muscle load on DRUJ stability. J Hand Surg 2003;28A:943–950.
24. Gordon KD, Pardo RD, Johnson JA, King GJ, Miller TA. Electromyographic activity and strength during maximum isometric pronation and supination efforts in healthy adults. J Orthop Res 2004; 22:208–213.
25. Dunning CE, Lindsay CS, Bicknell RT, Patterson SD, Johnson JA, King GJ. Supplemental pinning improves the stability of external fixation in distal radius fractures during simulated finger and forearm motion. J Hand Surg 1999;24A:992–1000.
26. Gofton WT, Gordon KD, Dunning CE, Johnson JA, King GJ. Soft-tissue stabilizers of the distal radioulnar joint: an in vitro kinematic study. J Hand Surg 2004;29A:423–431.
27. Schuind F, An KN, Berglund L, Rey R, Cooney WP III, Linscheid RL, et al. The distal radioulnar ligaments: a biomechanical study. J Hand Surg 1991;16A:1106–1114.
28. af Ekenstam F. Anatomy of the distal radioulnar joint. Clin Orthop Relat Res 1992;275:14–18.
29. Bade H, Strickling H, Rutt J. Restriction of movement in the proximal and distal radioulnar joints in postraumatic angulation and torsion of the radius. Aktuelle Traumatol 1991;21:274–278.
30. Pogue DJ, Viegas SF, Patterson RM, Peterson PD, Jenkins DK, Sweo TD, et al. Effects of distal radius fracture malunion on wrist joint mechanics. J Hand Surg 1990;15A:721–727.